Journal of Achievements in Materials and Manufacturing Engineering
VOLUME 59
ISSUE 2
August
2013

Hardmetals characterization by tribological means

S.F. Ścieszka*, W. Grzegorzek, M. Żołnierz
Transportation and Tribotechnology Division, Silesian University of Technology,
ul. Akademicka 2a, 44-100 Gliwice, Poland
* Corresponding e-mail address: stanislaw.scieszka@polsl.pl

Received 14.05.2013; published in revised form 01.08.2013

Manufacturing and processing

ABSTRACT

Purpose: The objectives of the paper are as follows. Firstly the presentation of new and reliable integrated testing method, in which conjoin action involving fracture and abrasion of hardmetals is carefully monitored and analysed, and secondly the evaluation of the empirical relationship between mass loss as a result of edge chipping during the initial transition stage of abrasive wear and fracture toughness in the form of formula.
Design/methodology/approach: The tests were performed in a purpose-built testing machine. The apparatus consists of the disc rotating in the cylindrical chamber under normal force. The specimen bars, made from the hardmetals are attached to the upper side of the disc. The results from this testing show that by using one apparatus and one shape of the test specimen it is possible to obtain a reliable rating of hardmetals.
Findings: The integrated testing method required a theoretical or empirical model which describes the relationship between fracture toughness, other mechanical properties and the test's fracture indicator. The best correlation received was for empirical model based on study on abrasive wear by lateral cracking.
Practical implications: The proposed method offers advantages when used in hardmetals development programmes to rank a large number of materials in terms of abrasion and fracture resistance.
Originality/value: The innovative method enables the evaluation of abrasion and fracture resistance, one shape of specimen, and one testing procedure.
Keywords: Tribotesting; Abrasion; Fracture; Hardmetal

Reference to this paper should be given in the following way:
S.F. Ścieszka, W. Grzegorzek, M. Żołnierz, Hardmetals characterization by tribological means, Journal of Achievements in Materials and Manufacturing Engineering 59/2 (2013) 86-98.

1. Introduction

It is clear that there is no such thing as an intrinsic friction property of a material [1, 2]. The same applies to other tribological material properties, such as wear resistance and abrasiveness. These properties are system properties [3], in which the given material is only one of the elements (Fig. 1). sections of the paper are given roughly which we wish you to adopt during the preparation of your paper.

Wear by hard particles is illustrated in Figure 1. Abrasive wear is caused by particles which are forced to slide and roll over the material surface [4]. It was found that the intensity of abrasive wear in such systems is significantly affected by the size reduction of abradant particles [5, 6]. This effect is attributed to individual particle collapse, the sudden release of elastic strain energy, and the formation of new sharp cutting edges as an additional source of damage. These arguments introduce the comminution of abrasive particles as an additional parameter that should be included in the tribological system.

Abrasive wear, illustrated in Figure 1 is very common in industrial and other activities. It prevails in mining; e.g. excavation, loading, haulage and drilling; in agriculture; e.g. plough narrow, and in mineral processing and handling systems. Abrasive wear is usually caused by hard mineral particles which

produce no significant adhesion and seizure phenomena during the process. The large variety of shapes and mechanical properties of the abrasive particles (e.g., quartz sand) and diverse loading, conditions give rise to variable stresses by contact.

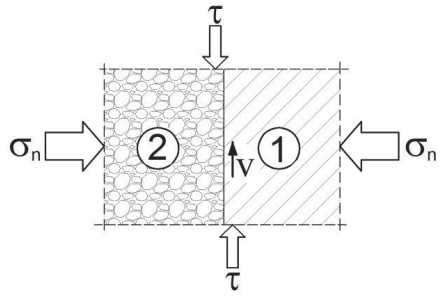

Fig. 1. Hard particles abrasion (laboratory scale process) or granular bulk solid abrasion (industrial scale process), where: 1 - material (first body), 2 - abradant particles (third body)

Wear debris is generated as a result of a single or multiple actions of the abrasive agents, i.e. microploughing, microcutting, microcracking and microfatigue. This diversity of wear processes and conditions results in various combinations of the elementary processes involving the disintegration and loosening of the surface layers.

Since the abrasive wear process is complex and varies from one situation to another, the performance of a material in tribological system can only be determined by a carefully designed simulation [2] in which mechanical elements undergo processes similar to those in a complex engineering environment. If e.g. the engineering environment includes processes such as abrasive wear of material and size reduction of abradant particles, both of these must be incorporated into the simulation. There is a complicated energy balance inside any tribo-mechanical system. Attrition, comminution and fracture processes result in energy conversion from one form to another, including such primary energy absorbing processes as the creation of new surfaces, plastic deformation, elastic deformation, vibration, and noise. In secondary energy dissipation processes, most of the energy expended in internal and external friction is converted to heat. Other factors influencing the above processes are environmental effects such as the presence of chemically active gases and vapours which e.g. affect the fracture processes [7,8]. The tribotesting system, which incorporates attrition, comminution and fracture processes, is shown in Figure 2.

In mineral processing e.g. inside the mill, the comminution process continues until all individual mineral particles are small enough to leave the mill. The energy consumed for such a particle to be produced from the initial charge is a function of the efficiency of the mill and a property of the mineral which determines the ease with which it is broken up. The empirical factor to determining the rate at which the comminution proceeds is represented by the index of comminution (IC) proposed in [9, 10]. The abrasiveness of a mineral (granular bulk solid) can be described by an abrasion factor (AF) and by an index of abrasion (IA).

In order to illustrate the advantage of the system approach to tribological problems within the complex tribo-mechanical system let us analyse the basic relations between the system's elements inside any mill, pulverizer or other mineral processing installation. Each of the above mentioned indices (IC, AF) measures a given property of the bulk solid mineral, but the wear in a mill is a composite of these two separate factors, since the easier it is to crush a mineral, the less time the particle will spend inside the mill, resulting in a lower overall wear rate.

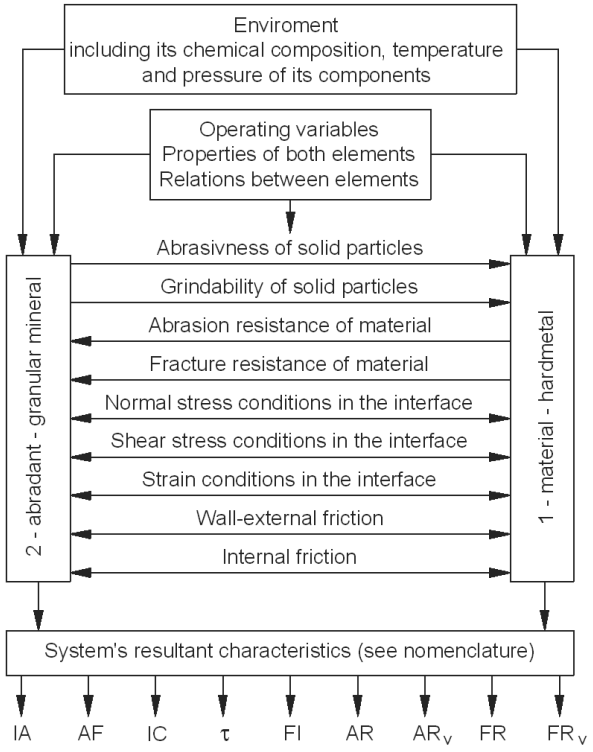

Fig. 2. Tribotesting system which includes abrasive interaction between material and solid particles, solid particles size reduction, material abrasion, and fracture

The method of testing presented in Figure 3 combines both comminution and wear. In this method any particle which reaches a predetermined size is ejected from the grinding area through the annulus between the grinding bar holder and the stationary cylinder.

In this method the shear process is accompanied by the wear of the bar. The grains of mineral become ground to a greater or lesser degree, which can be determined by the index of comminution (IC). This index characterises the ease of pulverisation of minerals. A prepared sample of mineral receives a given amount of grinding energy (energy input) and the change in size is determined by sieving. The index of comminution (IC) of mineral is expressed in milligrams of pulverized mineral (fraction below 75 μm particle size) per Joule energy input.

The relative displacement between the layers of particulate mineral and the bar's surface provides abrasive wear of the bar material due to mineral particles sliding across the surface. They may also move relative to one another and they may rotate while sliding across the wear surface. In an industrial situation, as well as in a laboratory test apparatus, high-stress abrasion occurs where hard particles are crushed. The abrasion property of

mineral is represented by the abrasion factor (AF). The abrasion factor (AF) is the mass of metals lost by abrasion from a carbon steel bar when rotated in a specified mass of mineral under specified conditions, expressed in milligrams of metal lost per kilogram of pulverized mineral.

Abrasion resistance (AR) and fracture resistance (FR) give the best indication of the material's resistance to abrasive wear and resistance to edge fracture. A complete set of calculation formulae is presented in the next chapters.

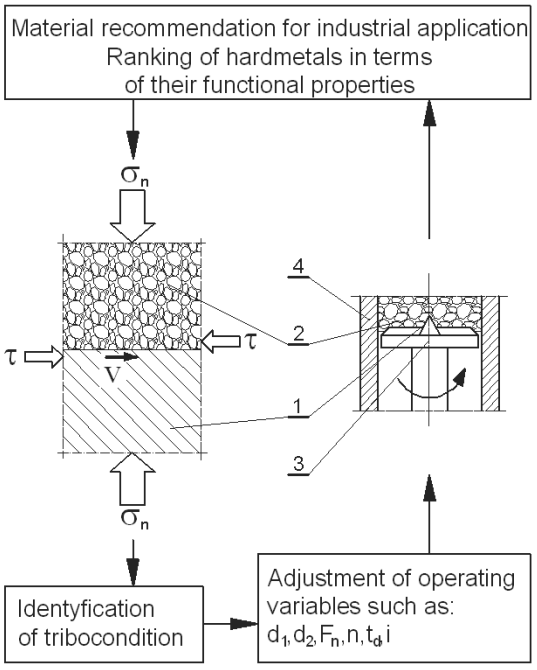

Fig. 3. Simulative tribo-testing of attrition, comminution, and fracture phenomena, where: 1 - material (hardmetal sample), 2 - abradant (granular bulk solid mineral), 3 - disc (bar holder), 4 - cylindrical chamber

In this paper a simple and reliable integrated testing method, in which conjoin actions involving fracture and abrasion of hardmetals together with abradant comminution is analysed. The presented system approach to tribotesting enables mechanical characterization of hardmetals in attrition contact with bulk solid minerals which take places in e.g. mineral processing or in drilling action.

2. Abradant or granular bulk solid mechanical characterization

2.1. Shear strength of granular bulk solid

The shear strength of a granular bulk solid is the maximum available resistance that it can offer to shear stress at a given point within itself. When this resistance is exceeded, continuous shear displacement takes place between two parts of the granular bulk solid. The shear strength of fine materials depends on three factors:

1) sliding friction between the adjacent grains;
2) rolling friction, as some of the grains will change position by rolling and
3) the resistance to the movement of individual grains, generally called the effect of interlocking action.

Interlocking is affected to some degree by particle shape and grain size distribution. A typical pattern of a granular bulk solid behaviour in a shear test is shown in Fig. 4.

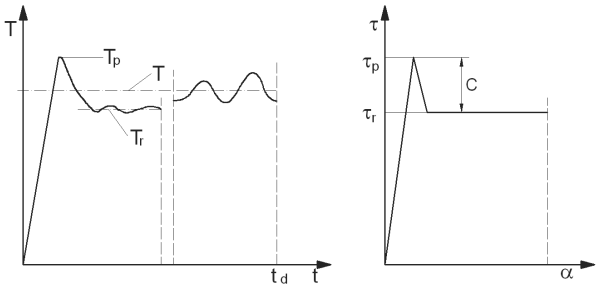

Fig. 4. Torque diagram (a) and schematic representation of fine cohesive material behaviour in a shear test (b). For non-cohesive materials component C→0 and $\tau_p=\tau_r$

The shear stress diagram consists of peak and residual values. After the peak value of torque is reached at a small value of angular displacement, the shear strength decreases and the torque necessary to continue the shear displacement is reduced to the final residual value of torque. Shear displacement takes place across a shear zone. Stress σ acting at any point within the plane of shear action can be resolved into two components: σ_n and τ.

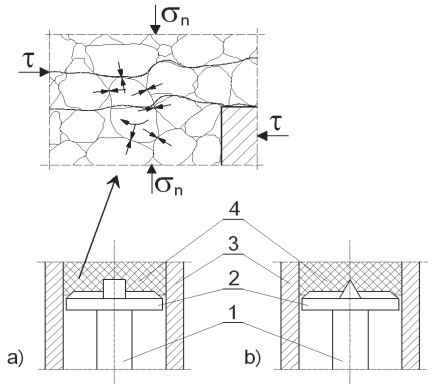

Fig. 5. Schematic diagram of arrangement inside the apparatus (fine mineral versus disc-bar assembly with two different shapes of bar: a) rectangular and b) triangular and interpretation of interaction between the granular mineral and the bar within shear zone, where: 1 - drive shaft, 2 - disc-bar assembly, 3 - cylindrical container, 4 - granular mineral-abradant. Bars with rectangular cross-section are intended for testing various coatings, while bars with triangular cross-section (which were used in this investigation) are meant for the evaluation of both abrasion and fracture resistance

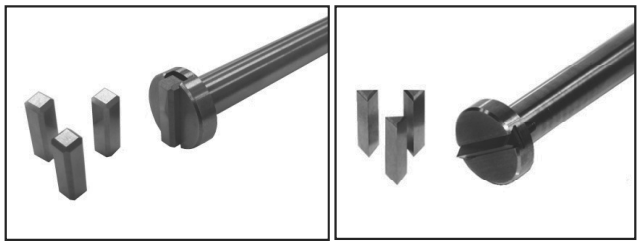

Fig. 6. The view of specimen holders, drive shaft and specimens

An examples of results from the experiments carried out in the proposed apparatus (Figs. 5-8) are shown in Table 1. The shear resistance can be evaluated from Coulomb's equation:

$$\tau_p = C + \sigma_n \tan\phi = \frac{3T_p}{2\pi R^3} \cdot 10^{-6} \ \text{(MPa)} \quad (1)$$

and

$$\tau_r = \sigma_n \tan\phi = \frac{3T_r}{2\pi R^3} \cdot 10^{-6} \ \text{(MPa)} \quad (2)$$

where T_p is the peak value of torque (Nm), C the apparent cohesion (MPa), T_r the residual value of torque (Nm), R the radius of cylinder (m), τ_p the peak value of shear strength (MPa), τ_r the residual value of shear strength (MPa), F_n the normal force (N), and $\sigma_n = \frac{F_n}{\pi R^2}$ the normal stress (MPa).

a)

b)

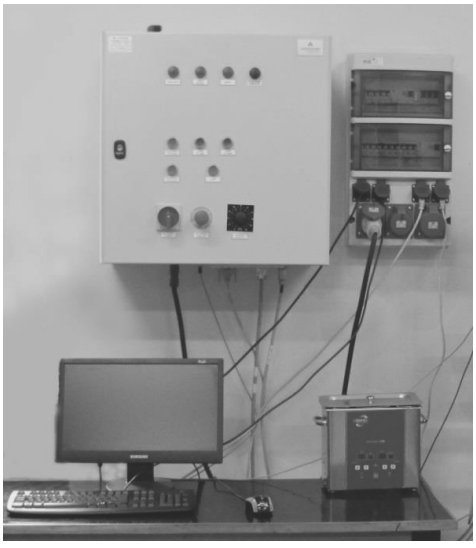

c)

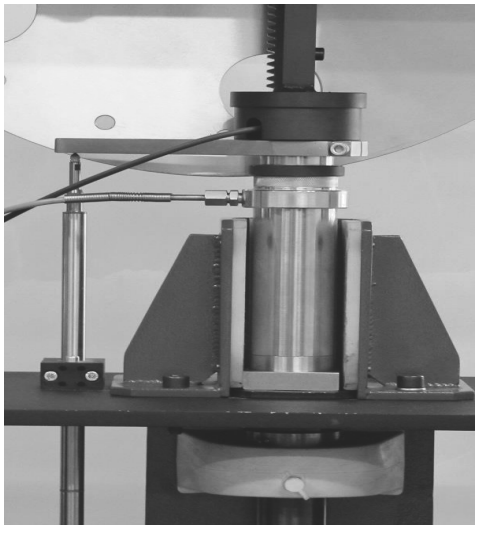

Fig. 7. The view of the apparatus built by the Institute for Sustainable Technology, Radom (a) with mounted cylindrical tribotester (c), and computer system for control and measurement (b)

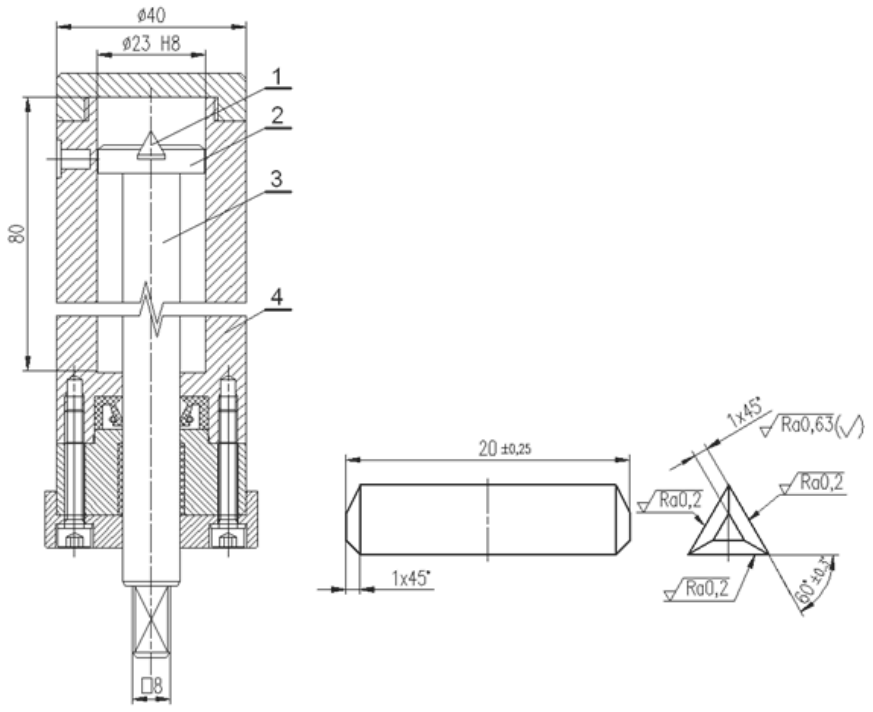

Fig. 8. Cylindrical tribotester (a), and bar-specimen (b) with triangular cross-section, where: 1-specimen, 2-disc-specimen holder, 3-drive shaft, 4-cylindrical container

In a body of fine bulk materials under normal stress the particles are in a state of static equilibrium. To displace them tangentially, it is necessary to overcome the resistance offered by the existing adhesive bonds between the particles, and by a considerable degree of interlocking (i.e. by the apparent cohesion). After a peak stress is reached at a small value of shear displacement, the degree of interlocking decreases and some of the adhesion bonds are ruptured. The shear necessary to continue shear displacement is reduced by approximately the value of apparent cohesion (Figs. 4 and 9). The decrease in the degree of interlocking is caused by the particles being crushed and broken and by the redistribution of the particles (sliding, rolling and lifting). The magnitude of internal resistance while shearing, i.e., internal frictional angle:

$$\phi = \arctan\frac{\tau_r}{\sigma_n} = \arctan\frac{3T_r}{2RF_n} \quad (\text{deg}) \tag{3}$$

depends on the grain size and environment e.g. moisture content. Therefore, consistent bulk solid sample preparation is important.

2.2. Grinding and abrasion action of granular bulk solid

The granular bulk solid size reduction process can be determined as presented in the previous chapter by the index of comminution (IC). Relative displacement between the layers of fine bulk solid and the bar's surface as in Figure 5 provides considerable abrasion wear of the bar material due to bulk solid grains sliding across the surface.

The abrasion property of bulk solids is represented by the abrasion factor (AF) and the index of abrasion (IA).

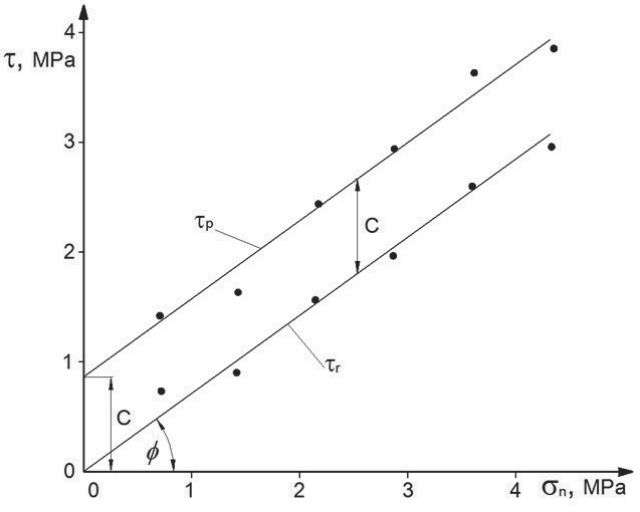

Fig. 9. Shear strength of fine coal as function of normal stress, and Coulomb's parameters ϕ and C (Equation 1)

The above described properties can be calculated as follows [11]:

$$IC = \frac{PC}{EI} \tag{4}$$

where IC is the index of comminution (mg/J), PC the mass of pulverized abradant that is less than 75μm (mg), EI the energy input (J).

$$AF = \frac{\Delta m}{PC} \cdot 10^6 \tag{5}$$

where AF is the abrasion factor (mg/kg), Δm the wear of bar (mg).

$$IA = \frac{\Delta m}{S_A \cdot t_d} \tag{6}$$

where IA is the index of abrasion (mg/m^{2}s) S_A the area of surface exposed to abrasion (m^2), t_d the duration of test (s).

The use of the proposed method leads to the determination of a number of parameters of interest in mineral processing and bulk solid handling.

A series of tests have been performed on one coal, coal water slurry and three abradants. The results are summarized in Table 1.

The proposed method is much more flexible than the standard method [12], and it may simulate quite closely attrition conditions inside various mineral processing systems and bulk solid handling equipment such as mill, chute and conveyor. The method also allows for a quick and inexpensive determination of the abrasiveness and grindability of bulk solid in any operational condition (viz. pressure, sliding velocity and temperature) and in any material configuration (viz. material of bar and sample of particulate material-abradant). In the proposed method a sample of only about 20 g of abradant (range of particles size 600-1200μm) was used and normal loading, F_n=1000 N was applied.

Table 1.
Basic mechanical properties of selected bulk solids (abradant)

Properties	Coal	Coal water slurry	SiO_2 99 wt.%	Al_2O_3 99 wt.%	SiC 99 wt.%
Vicker's hardness (HV)	~65	-	~970	~1500	~2500
Shear strength $\tau=\tau_r$ (MPa)	1.58	0.833	2.58	2.99	2.97
Apparent cohesion C (MPa)	1.11	1.49	~0	~0	~0
Internal friction angle Φ(deg)	33.4	19.1	53.1	55.8	55.4
Index of comminution IC (mg/J)	0.512	0.491	2.030	1.792	1.858
Abrasion factor AF (mg/kg)	69	33	140	437	2655
Index of abrasion IA (mg/m^{2}s)	39	11	111	403	2253

The abrasiveness of bulk materials (AF and IA) tested in various material configurations (with various bar materials) will show relatively different results. Therefore the abrasive property of bulk material should be tested with bars made from materials currently used or considered for use in the equipment. Only results from tests which completely simulate operational and material conditions in the industrial installation can be directly applied to design calculations. In the tests presented in Table 1 BWC2 hardmetal bars were used (Table 4).

3. Method for hardmetals mechanical characterization

The fracture toughness is often the major limiting parameter governing the use of hard materials tools. Hence there is a need for research aimed at increasing toughness without sacrificing wear resistance. To aid in this objective, a simple and reliable integrated testing method, in which a conjoin action involving both fracture and abrasion is needed. One such method currently being developed is presented in this paper. The method is based on the concept of edge chipping during the initial transition stage of abrasion wear, which is controlled by a brittle fracture process (Figs. 3, 5 and 7). Fracture toughness and wear resistance are two of the major material characteristics to take into consideration when designing components such as tools made of hardmetals. This is mainly due to the risk of brittle fracture in the tools in high contact pressure conditions. Rock drilling and cutting produce both impact and abrasion in various relative amounts at the tool/rock interface mainly because the rock fragmentation itself is a discrete process rather than a continuous one [13].

3.1. Toughness evaluation based on edge damage pattern

When a load is applied along the sharp edge of hard and brittle tools or various other construction elements, cracks may initiate, propagate and eventually spall from the surface. On the other hand, in grinding or machining of brittle materials such as ceramics, optical glasses and hardmetals etc., flaking or chipping are often seen at the work edge where the cutting edge comes into contact with or separates from the work-piece. This edge damage on the tools and on the work-pieces has been identified as a technologically significant problem in e.g. edge machining, edge mounting etc, and was named as edge cracking, edge spalling, edge flaking, and edge chipping [15]. A number of attempts were made to devise novel methods of testing for a pragmatic way of ranking materials for toughness [14, 15] based on edge damage controlled by fast fracture.

The controlled combined action of a granular hard abradant both as a multipoint source for loading the sample of hard material in the vicinity of the edge and as a hard, angular abradant can be used for ranking materials for both toughness and for wear resistance (Figs. 2 and 3). This combined action takes place within a cylindrical chamber filled with granular abradant in which normal stress, σ_n, (Equation 2) is controlled by external loading F_n. External torque, T, applied to the drive shaft is used to overcome the shear resistance of the granular abradant and friction resistance on the interface.

The method which enables simultaneous brittle fracture and abrasion testing allows for simulation of stress and sliding speed conditions found e.g. between drills and rock. But in fact any material combination (i.e. material of bar-sample or granular abradant-mineral sample) can be used under any operating condition (i.e. normal stress, sliding velocity and temperature). Another advantage of the tribotester itself is that the ground abradant - granular bulk solid is allowed to leave the attrition area through the gap between a disc and a wall of the cylindrical chamber as occurs in actual drilling or grinding. The apparatus consists of the disc rotating in the cylindrical chamber under normal force. The specimen bars are attached to the upper side of the disc (Figs. 6 and 8). The specimen bars are made from the hardmetals being tested. The test procedure, overall set-up of the tribotester, the method of calculation and presentation of the results were described in details elsewhere [14, 15].

The tests were performed in a purpose-built testing machine. The overall view in Figure 7 shows the apparatus with the mounted cylindrical tribotester and loading pulley. Specification of the apparatus and experimental details are shown in Table 2.

Test samples (Figs. 6 and 8) were prepared in accordance with design specifications [16]. The hardmetal testpieces were prepared by careful grinding. Test edges were not chamfered. The hardmetals and their properties are summarized in Tables 3 and 4.

The preliminary results revealed that the edge chipping process (the fracture controlled transition wear process) was taking place only during the first 15 revolutions.

Table 2.
Specification of the apparatus and experimental details

Name	Edge abrasion tribotester
Normal load (N)	1000
Normal stress (MPa)	2.4
Drive shaft speed (rpm)	30
Test duration (number of rev.)	15
Mean sliding distance (m)	0.471
Abradant A - Fused alumina (Al_2O_3)	600-1200 μm
Abradant B - Quartz sand (SiO_2)	600-1200 μm

Table 3.
Hardmetals composition tested with alumina abradant and their mechanical specification (manufacturer's data, laboratory internal hardmetal's grade denotation)

No	Hardmetal grade	Composition (wt.%)			ρ (Mgm^{-3})	E (GPa)	K_C ($MPam^{½}$)	Hardness HV_{30}
		WC	TiC+TaC+NbC+VC	Co,Ni				
1	AWC1	90	-	10	14.52	590	10.02	1543
2	AWC2	90	1	9	14.37	580	9.52	1589
3	AWC3	90	2	8	14.55	590	10.08	1679
4	AWC4	96.7	-	3.3	15.32	620	8.20	2071
5	AWC5	80	-	20	13.53	480	35.70	890
6	AWC6	75	-	25	13.11	440	42.70	804

Table 4.
Hardmetals composition tested with quartz sand abradant and their mechanical specification (manufacturer's data, laboratory internal hardmetal's grade denotation)

No	Hardmetal grade	Composition (wt.%)			ρ (Mgm^{-3})	E (GPa)	K_C ($MPam^{½}$)	Hardness HV_{30}
		WC	TiC+TaC+NbC+VC	Co,Ni				
1	BWC1	91	-	9	14.6	590	17	1250
2	BWC2	94	-	6	14.9	610	14	1430
3	BWC3	85	-	15	14.0	540	18	1150
4	BWC4	94	-	6	14.9	640	11	1600
5	BWC5	93.8	0.2	6	14.9	630	10	1800
6	BWC6	87	5	8	13.4	520	13	1500

3.2. Experimental procedure

In the final part of the investigation all the materials listed in Tables 3 and 4 were tested. The test procedure developed during the previous study and presented in [14, 15] was applied. The procedure consisted of three or five consecutive tests lasting 15 revolutions, but only the first one starting with a sharp sample edge. This test procedure was repeated at least six times for every material tested. In every test only one normal load equalling 1000N was applied.

In this part of the investigation the following notations and calculations were used:

$$\Delta\overline{m}_1 = \frac{1}{n}\sum_{1}^{n}\Delta m_1 \tag{7}$$

where $\Delta\overline{m}_1$ is the mass loss during the first tests repeated each time with new sharp sample edges (mg), n the number of edges tested, Δm_1 the mass loss during the first test (the first of three or five consecutive tests starting with unworn sharp edges) lasting 15 revolutions (mg).

$$\Delta\overline{m}^{a} = \frac{1}{2n}\sum_{1}^{2n}\Delta m \tag{8}$$

where $\Delta\overline{m}^{a}$ is the mass loss during tests other than the first ones (tested two or four times) each lasting 15 revolutions. It represents mass loss controlled by stable-abrasion mode of wear after the transition-fracture controlled mode of wear was completed (mg).

$$\Delta\overline{m}^{F} = \Delta\overline{m}_1 - \Delta\overline{m}^{a} \tag{9}$$

where $\Delta\overline{m}^{F}$ is the mass loss solely as a result of fracture (edge chipping) during the first tests (mg).

$$\Delta\overline{V}_1 = \frac{\Delta\overline{m}_1}{\rho} \tag{10}$$

where $\Delta\overline{V}_1$ is the volumetric material loss (mm^3), ρ the density (mg/mm^3).

$$\Delta\overline{V}_a = \frac{\Delta\overline{m}^{a}}{\rho} \tag{11}$$

where $\Delta\overline{V}_a$ is the volumetric material loss by abrasion (mm^3).

$$\Delta\overline{V}_F = \frac{\Delta\overline{m}^{F}}{\rho} \tag{12}$$

where $\Delta\overline{V}_F$ is the volumetric material loss by fracture (mm^3).

$$AR = \frac{15}{\Delta\overline{m}^{a}} \tag{13}$$

where AR is the abrasion resistance (rev/mg).

$$AR_V = \frac{15}{\Delta\overline{V}_a} \tag{14}$$

where AR_V is the volumetric abrasion resistance (rev/mm^3).

$$FR = \frac{15}{\Delta\overline{m}^{F}} \tag{15}$$

where FR is the fracture resistance (rev/mg).

$$FR_V = \frac{15}{\Delta\overline{V}_F} \tag{16}$$

where FR_V is the volumetric fracture resistance (rev/mm^3).

$$FI = \frac{\Delta\overline{m}^{F}}{\Delta\overline{m}_1} = \frac{\Delta\overline{V}_F}{\Delta\overline{V}_1} \tag{17}$$

where FI is the fracture index.

The value of equivalent fracture surface S in mm^2 was calculated from $\Delta\overline{V}_F$ (mean volume loss solely as a result of fracture-edge chipping during the first tests) assuming that the crack surface produced during the test is flat and parallel to one side of the sample (prism), i.e.

$$S = \left(\frac{2\cdot\Delta\overline{V}_F\cdot l}{\sin 60°}\right)^{\frac{1}{2}} \tag{18}$$

where l is the length of the edge (mm).

The procedure presented above is based on the distinction between initial processes (tribological transition) controlled by fracture edge damage and the steady stage of wearing predominantly controlled by microabrasive wear mechanisms.

The steady stage of wearing yields a rating of the wear resistance of materials. In steady-state wear, the spread of results was remarkably small, which when combined with the very accurate mass-loss measurement, makes the method very discriminating.

The method presented above does not produce the fracture toughness value (e.g. K_{IC}) as directly as the standardised plain strain fracture toughness tests do. The integrated testing method requires the theoretical or empirical models (formulae) which describe the relationship between fracture toughness and other mechanical properties. These formulae are usually based on well established assumptions and laws such as energy balance, the Hertzian stress distribution, or on empirical and semi-empirical relationships which were proved to be valid in the specified range [4,7,15, 17-19].

In accordance with the objectives of the present work shown in the introduction, the following formulae are proposed for further study and the least square fit evaluation (the dimensional analysis was used to modify all the following formulae in order to obtain the dimensional conformity between both sides of the equations):

a) Relationship applied in previous investigations by Scieszka and Filipowicz [17]

$$K_C = \alpha\left(\frac{E}{H}\right)\left(\frac{1}{S}\right)(EI \cdot F_n)^{\frac{1}{2}} \tag{19}$$

where α is the constant, E the modulus of elasticity (GPa), H the hardness (MPa).

b) Relationship based on Hornbogen study [18]

According to Hornbogen, the transition from the unsteady to the steady stage of wear is equivalent to the change in probability of wear particle formation. This probability can be related to the plastic strain ε_p produced during an asperity interaction, and the critical strain ε_c, at which cracks start to propagate in the material. In $\varepsilon_p > \varepsilon_c$ there is an increased probability of wear particle formation by fragmentation, hence wear rate depends on the fracture toughness and hence

$$K_C = \beta\left(\frac{E^2}{H}\right)^{\frac{1}{4}}\left(\frac{1}{S}\right)^{\frac{1}{2}} F_n^{\frac{3}{4}} \tag{20}$$

where β is the constant.

c) Relationship based on the empirical model presented in [4] for the abrasive wear by brittle fracture which consists of the removal of material by lateral cracking. Hence

$$K_C = \gamma\left(\frac{E}{H}\right)^2\left(\frac{1}{S}\right)^2\left(\frac{1}{H}\right)^{\frac{5}{4}} F_n^{\frac{9}{4}} \tag{21}$$

where γ is the constant.

d) Relationship based on Hussainova study [19] on erosive wear of hard materials. Hence

$$K_C = \delta\left(\frac{E}{H}\right)\tau_r\left(\frac{l^{\frac{3}{2}}}{S^{\frac{1}{2}}}\right) \tag{22}$$

where δ is the constant, τ_r the shear strength of abradant (MPa), l the length of the edge (mm).

The results from the final part of the investigation were summarised in Tables 3 to 8.

The results show that by using one apparatus, one shape of test specimen, and only one relatively easy testing procedure it is possible to obtain a reliable rating of hardmetals according to both criteria, i.e. their edge fracture toughness as well as their resistance to abrasive wear in rubbing contact with particulate alumina and sand.

Table 5.
Results from tests run at normal load, F_n = 1000 N and individual consecutive test duration, i = 15 revolutions (with alumina abradant)

No	Hardmetal grade	Test results: arithmetic mean values and standard deviations												
		$\Delta\overline{m}_l$		$\Delta\overline{m}^a$		$\Delta\overline{m}^F$		$\Delta\overline{V}_l$		$\Delta\overline{V}_a$		$\Delta\overline{V}_F$		S_a
		(mg)		(mg)		(mg)		(mm^3)		(mm^3)		(mm^3)		(mm^2)
1	AWC1	0.647	0.057	0.246	0.012	0.401	0.063	0.0445	0.0039	0.0169	0.0008	0.0276	0.0043	1.071
2	AWC2	0.542	0.021	0.217	0.012	0.325	0.034	0.0377	0.0014	0.0151	0.0008	0.0226	0.0023	0.969
3	AWC3	0.805	0.088	0.118	0.016	0.686	0.072	0.0553	0.0060	0.0081	0.0011	0.0471	0.0049	1.399
4	AWC4	0.966	0.258	0.123	0.013	0.843	0.251	0.0630	0.0168	0.0080	0.0008	0.0550	0.0164	1.512
5	AWC5	2.087	0.093	1.826	0.043	0.261	0.102	0.1542	0.0068	0.1349	0.0031	0.0192	0.0075	0.893
6	AWC6	2.193	0.057	1.999	0.078	0.191	0.092	0.1672	0.0043	0.1524	0.0059	0.0145	0.0070	0.776

Table 6.
Property indicators calculated from test results run at normal load, F_n = 1000 N and individual consecutive test duration, i = 15 revolutions (with alumina abradant)

No	Hardmetal grade	Test results: arithmetic mean and standard deviation									
		AR		AR_V		FI		FR		FR_V	
		(rev/mg)		(rev/mm^3)		-		(rev/mg)		(rev/mm^3)	
1	AWC1	60.9	4.0	884.2	58.1	0.616	0.044	37.4	6.0	543.0	87.1
2	AWC2	69.12	4.0	993.2	57.5	0.599	0.039	46.15	5.0	663.2	71.8
3	AWC3	127.1	17.0	1842.9	247.3	0.852	0.004	21.86	2.27	318.1	33.0
4	AWC4	121.1	13.8	1867.5	211.4	0.872	0.037	17.79	6.62	272.5	101.4
5	AWC5	8.21	0.22	111.1	2.9	0.125	0.042	57.47	24.48	777.6	331.2
6	AWC6	7.50	0.30	98.3	3.9	0.087	0.041	78.53	37.80	1029.5	495.5

Table 7.
Results from tests run at normal load, F_n = 1000 N and individual consecutive test duration, i = 15 revolutions (with sand abradant)

No	Hardmetal grade	Test results: arithmetic mean values and standard deviations												
		$\Delta\overline{m}_I$		$\Delta\overline{m}^a$		$\Delta\overline{m}^F$		$\Delta\overline{V}_I$		$\Delta\overline{V}_a$		$\Delta\overline{V}_F$		S_S
		(mg)		(mg)		(mg)		(mm^3)		(mm^3)		(mm^3)		(mm^2)
1	BWC1	0.66	0.080	0.30	0.032	0.36	0.086	0.05	0.005	0.02	0.002	0.02	0.006	1.011
2	BWC2	0.79	0.048	0.26	0.019	0.54	0.052	0.06	0.003	0.02	0.003	0.05	0.003	1.225
3	BWC3	0.73	0.038	0.40	0.044	0.33	0.058	0.05	0.006	0.03	0.004	0.02	0.005	0.990
4	BWC4	1.40	0.064	0.14	0.027	1.25	0.069	0.09	0.010	0.01	0.002	0.08	0.010	1.876
5	BWC5	2.51	0.179	0.69	0.134	1.82	0.223	0.17	0.021	0.05	0.010	0.12	0.019	2.258
6	BWC6	1.40	0.078	0.24	0.032	1.17	0.084	0.10	0.012	0.02	0.003	0.09	0.011	1.902

Table 8.
Property indicators calculated from test results run at normal load, F_n = 1000 N and individual consecutive test duration, i = 15 revolutions (with sand abradant)

No	Hardmetal grade	Test results: arithmetic mean and standard deviation									
		AR		AR_V		FI		FR		FR_V	
		(rev/mg)		(rev/mm^3)		-		(rev/mg)		(rev/mm^3)	
1	BWC1	49.32	6.167	720.00	48.050	0.54	0.137	41.76	4.541	609.74	40.835
2	BWC2	58.63	5.920	873.62	58.271	0.68	0.073	27.91	2.357	415.81	27.799
3	BWC3	37.82	4.888	529.41	35.365	0.45	0.082	45.45	4.028	636.36	42.534
4	BWC4	104.65	20.741	1548.84	103.305	0.90	0.075	11.97	1.148	177.13	11.932
5	BWC5	21.77	4.464	323.22	21.795	0.73	0.157	8.24	1.920	122.33	8.494
6	BWC6	63.16	9.382	846.32	56.476	0.83	0.088	12.87	1.381	172.41	11.642

Assuming that testing with sand as the abradant is a standard condition of testing, one can recalculate (or standardized) the results obtained from other tests, e.g. tests with alumina as abradant by the following equations

$$FR_S \cong \frac{\tau_a}{\tau_s} \cdot FR_a \quad (23)$$

$$AR_S \cong \frac{IA_a}{IA_s} \cdot AR_a \quad (24)$$

$$FI_S \cong \frac{\tau_s}{\tau_a} \cdot FI_a \quad (25)$$

$$S_S \cong \sqrt{\frac{\tau_s}{\tau_a}} \cdot S_a \quad (26)$$

where τ_s is the shear strength of sand (Table 1), τ_a the shear strength of alumina (Table 1), IA_s the index of abrasion for sand (Table 1), IA_a the index of abrasion for alumina (Table 1), S_a the equivalent fracture surface for alumina (Table 5), S_s the equivalent fracture surface for sand (Table 7), AR_s the abrasion resistance for sand (Table 8), AR_a the abrasion resistance for alumina (Table 6), FR_s the fracture resistance for sand (Table 8), FR_a the fracture resistance for alumina (Table 6), FI_s the fracture index for sand (Table 8), FI_a the fracture index for alumina (Table 6).

Examination of the selected new and worn edges, at various stages of the test procedure was conducted. SEM observations of the new, unworn samples revealed the quality of the surface finish obtained by grinding and the surface scars representative for the edge tip area. The morphology of ground surfaces together with unworn edges are depicted in Figure 10. SEM micrographs show microploughing furrows and microcuttings both parallel to the edge. Occasionally, abrasion grits from the grinding wheel were found embedded into the specimen's surface.

As the surface roughness in the vicinity of the edge and particularly the crack-like defects generated by the grinding process such as sharp microcutting and microcracking contribute to the fracture controlled mass loss, it is essential that all the

samples have statistically similar surface morphology. The original, almost intact surface morphology was found of the test procedure on the trailing side of every sample. This was recorded on the hardmetal AWC5 (Fig. 12a).

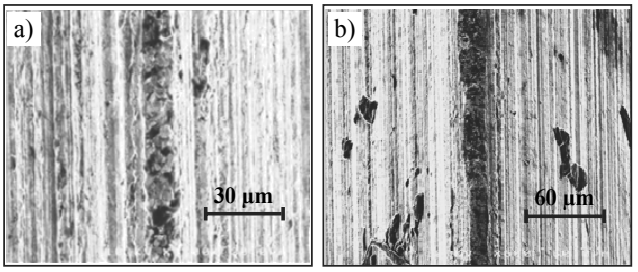

Fig. 10. SEM micrographs of the unworn samples showing grinding scars on both sides of the edge and the edge tip width: a) AWC5, b) AWC4

Figure 11 presents a typical fracture surface of the submicron grained hardmetal (AWC4) with some embedded carbide grains protruding from the phase and the others being removed, exposing the sockets that contained them. For this hardmetal the crack propagation was primarily along WC-Co interfaces with a partially transgranular fracture through the cobalt matrix.

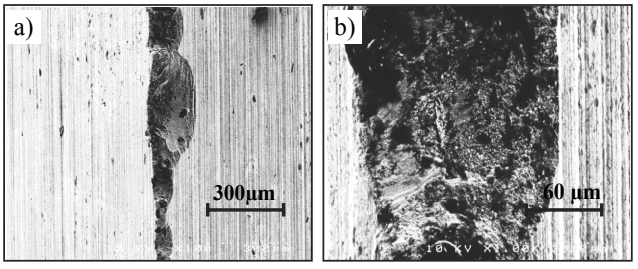

Fig. 11. SEM micrographs of two different hardmetals after only two revolutions showing the early stage of edge fracture controlled wear: a) AWC4, a typical edge chipping and abrasion damages on leading (left) side of the edge, b) AWC4, surface created by intergranular fracture partly reshaped by abrasion action of alumina particles on leading side of the edge

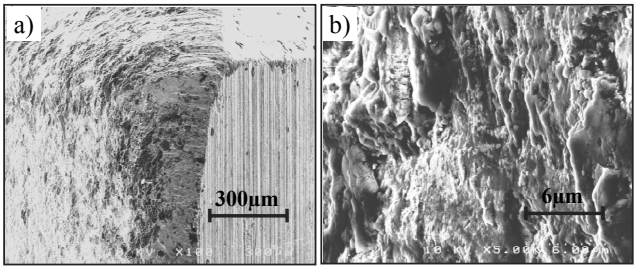

Fig. 12. SEM micrographs of the hardmetal AWC5 worn sample after the full test (45 revolutions): a) the edge at its extremity showing the difference between the leading (left) and trailing (right) side, b) abrasion damages on the leading side

Surface worn by the abrasion action of alumina particles such as the hardmetal AWC5 sample after the full test is presented in Figure 12. The wear mechanisms include such abrasion controlled stages as: extrusion of cobalt binder, cracking of the carbide grains, WC grains breaking into small fragments, and finally the small fragments gradual removal. The above wear mechanisms were investigated separately in stepwise abrasion tests and are described in [15].

The proposed simultaneous abrasion and fracture testing, as well as the final experimental results presented and discussed in this paper clearly indicate that the method offers some potential advantages when it is used in a hardmetals development programme to rank a large number of materials in terms of wear and fracture resistance [19,20]. For such, the programme's conventional evaluation methods (e.g. ISO 12962/ASTMB611, bulk fracture toughness methods) are less convenient as they require two different shapes of the specimens.

There is an emerging need for a reliable and cost effective ranking in terms of performance properties of the novel hard materials coming in as a result of the introduction new innovative processing technique.

Table 9.
The coefficient of correlation R values, for various equations and relationships

Equation and relationship	Tests with alumina	Tests with sand	Number of equation
$K_C = \alpha\left(\frac{E}{H}\right)\left(\frac{1}{S}\right)(EI \cdot F_n)^{\frac{1}{2}}$	0.911	0.895	(19)
$K_C = \beta\left(\frac{E^2}{H}\right)^{\frac{1}{4}}\left(\frac{1}{S}\right)^{\frac{1}{2}} F_n^{\frac{3}{4}}$	0.699	0.829	(20)
$K_C = \gamma\left(\frac{E}{H}\right)^2\left(\frac{1}{S}\right)^2\left(\frac{1}{H}\right)^{\frac{5}{4}} F_n^{\frac{9}{4}}$	0.975	0.925	(21)
$K_C = \delta\left(\frac{E}{H}\right)\tau_r\left(\frac{l^{\frac{3}{2}}}{S^{\frac{1}{2}}}\right)$	0.899	0.915	(22)
K_C vs. FR	0.782	0.943	(15)
K_C vs. FR_V	0.738	0.922	(16)
K_C vs. FI	0.891	0.731	(17)

Over the last 10 years, there has been a strong development of the novel approach leading to hardmetal microstructure with much higher resistance to fracture than normal, without sacrificing wear resistance. One developed approach leads to a microstructure with cellular architecture with the ability to stop or delay the propagation of microcracks [21]. The interior of the

cells has a low-carbon abrasion-resistant WC/Co composition, whilst the relatively thin walls are of high-cobalt, coarser, more fracture-resistant carbide. The above microstructure is an example of several functionally designed composite cemented carbides with distinctively anisotropic properties. To this category belong the established DC carbide, a so-called "double cemented" carbide in which pre-sintered granules of WC/Co hardmetal, of 2-4 μm grain size, are embedded in a pure cobalt matrix. DC carbide can be described as a "composite within a composite" that exhibits a superior combination of fracture toughness and high-stress wear resistance to conventional cemented carbide [22].

Another unconventional approach that produces a material that significantly exceeds the wear resistance and toughness of current metal cutting and forming tools has been demonstrated by Tough-Coated Hard Powders (TCHP) [23], and hard gradient coatings deposited on the tool materials [24-26].

Perhaps the most pronounced trend of the past years in the hardmetal industry has been a strong tendency towards finer and finer grained hardmetals.

The method and the indicators of functional wear resistance and toughness presented above have the potential to meet the development's test demands.

In the last stage of the investigation, the attempt was made to evaluate the empirical relationship between wear as a result of edge chipping during the initial transition stage of abrasion wear and fracture toughness in the form of formulae. The values of the coefficient of the correlation R for various equations and relationships are presented in Table 9.

4. Conclusions

The abrasive wear process is complex and varies from one situation to another. A material's performance for such tribological system can only be determined by a carefully designed simulation in which mechanical elements undergo processes similar to those in a complex engineering environment. If e.g. the engineering environment includes processes such as abrasive wear and fracture of material, and size reduction of abradant particles all these processes must be incorporated into the simulation.

The proposed simultaneous abrasion and fracture resistance testing method and procedure offer potential advantages when used in a hardmetals development programme to rank a large number of materials in terms of their above mentioned functional properties.

The method enables the evaluation of both abrasion and fracture resistance using only one apparatus, one shape of specimen and one testing procedure. The method is based on the finding that the wear transition stage, typical for the early and unsteady stage of the wearing process is controlled by brittle fracture while the following steady-state stage is controlled by the abrasion process.

Because the sample's surface quality, particularly crack-like defects, reduces a material's fracture strength and contributes towards edge chipping, it is recommended that only one kind of final surface finish procedure for all samples be applied. It is also recommended to measure and characterise the surface quality using profilometry.

The method of testing presented in the paper does not produce the fracture toughness value (e.g. K_c) as directly as the standardised plain strain fracture toughness test.

$$K_C = 189\left(\frac{E}{H}\right)^2\left(\frac{1}{S}\right)^2\left(\frac{1}{H}\right)^{\frac{5}{4}} F_n{}^{\frac{9}{4}} \qquad (27)$$

The integrated testing method requires the theoretical or empirical models (formulae) which describe the relationship between fracture toughness and other mechanical properties. For the range of materials tested, the best correlation (the coefficient of correlation, R^2=0.9594) was received for the empirical model based on Hutchings study on abrasive wear by brittle fracture and the removal of material by the lateral crashing.

Acknowledgements

The authors gratefully acknowledge the financial support of this research by the European Commission, Marie Curie Proposal: MCF1-2001-01159, Contract G5TR-CT-2002-00088. The authors also express his sincere appreciation to Drs. Mark Gee, Roger Morrell, Brian Roebuck and Andrew Gant from National Physical Laboratory, Teddington for their kind assistance. The authors would also like to thank the Institute for Sustainable Technology, Radom for building the tribotester as part of Innovative Economy Operational Programme.

References

[1] M. Godet, Tribo-Testing, P.B. Senholzi ed., Martinus Nijhoff Publishers, The Hague 1982, 535-609.
[2] M. Godet, Extrapolation in tribology, Wear 77 (1982) 29-44.
[3] H. Chichos, Tribology a system approach to the science and technology of friction, lubrication and wear, Tribology Series 8, 1978.
[4] I.M. Hutchings, Tribology friction and wear of engineering materials, Edward Arnold, London 1992.
[5] S.F. Ścieszka, A.S.M. Jadi, The effect of abradant particle commination on the intesity of three-body abrasion, Tribotest 5-2 (1998) 145-155.
[6] S.F. Ścieszka, Laboratory method for combined testing of abrasiveness, grindability and wear in mineral processing systems, Preprint 1991-AM-5F-1, STLE, 1-10.
[7] I.M. Hutchings, Wear by particulates, Chemical Engineering Science 42 (1987) 869-878.
[8] P.A. Rehbinder, E.D. Shchukin, Surface phenomena in solid during deformation and fracture processes, Pergamon Press, London, 1973.
[9] S.F. Ścieszka, A technique to investigate pulverizing properties of coal, Powder Technology 43 (1985) 89-102.
[10] S.F. Ścieszka, New concept for determining pulverizing properties of coal, Fuel 64 (1985) 1132-1142.
[11] S.F. Ścieszka, R.K. Dutkiewicz, Testing abrasive wear in mineral commination, International Journal of Mineral Processing 32 (1991) 81-109.

[12] ASTM Designation: G65-94, Standard test method for measuring abrasion using the dry sand/rubber wheel apparatus.
[13] J. Larsen-Basse, Wear transition of hardmetals in rock drilling, Powder Metallurgy 16/1 (1973) 1-32.
[14] S.F. Ścieszka, Wear transition as a mean of fracture toughness evaluation of hardmetals, Tribology Letters 11/3-4 (2001) 185-194.
[15] S.F. Ścieszka, Simultaneous abrasion and edge fracture resistance estimation of hard materials by the tribotesting method, Scientific Problems of Machines Operation and Maintenance 2/166 (2011) 55-104.
[16] S.F. Ścieszka, Abrasion and edge fracture resistance estimation of hard materials by tribotesting method, Tribotest 13 (2007) 103-113.
[17] S.F. Ścieszka, K. Filipowicz, An integrated testing method for cermet abrasion resistance and fracture toughness evaluation, Wear 216 (1998) 202-210.
[18] E. Hornbogen, The role of fracture toughness in wear of materials, Wear 33 (1975) 251-259.
[19] M. Szutkowska, Fracture toughness of advanced alumina ceramics and alumina matrix composites used for cutting tool edges, Journal of Achievements in Materials and Manufacturing Engineering 54/2 (2012) 201-210.
[20] M. Adamiak, J. Górka, T. Kik, Comparison of abrasion resistance of selected constructional materials, Journal of Achievements in Materials and Manufacturing Engineering 37/2 (2009) 375-380.
[21] K. Brookes, Novel approaches lead to better wear resistance in hard materials, Metal Powder Report 11 (2003) 34-39.
[22] Z. Fang, A. Griffo, B. White, G. Lockwood, D. Belnap, J. Bitter, Fracture resistant super hard materials and hardmetals composite with functionally designed microstructure, International Journal of Refractory Metals and Hard Materials 19 (2001) 453-459.
[23] R. Toth, J. Keanne, Tough coats on hard powders-a revolution in the making?, Metal Powder Report 9 (2003) 14-20.
[24] K. Gołombek, L.A. Dobrzański, Hard and wear resistance coatings for cutting tools, Journal of Achivements in Materials and Manufacturing Engineering 24/2 (2007) 107-110.
[25] L.A. Dobrzański, L.W. Żukowska, Structure and properties of gradient PVD coatings deposited on the sintered tool materials, Journal of Achivements in Materials and Manufacturing Engineering 44/2 (2011) 115-139.
[26] L.A. Dobrzański, M. Staszak, PVD and CVD gradient coatings on sintered carbides and sialon tool ceramics, Journal of Achivements in Materials and Manufacturing Engineering 43/2 (2010) 552-576.

Nomenclatures

AF - abrasion factor (mg kg^{-1})
AR - abrasion resistance (rev mg^{-1})
AR_v - volumetric abrasion resistance (rev mm^{-3})
C - apparent cohesion (MPa)
d_1 - diameter of disc (m)
d_2 - diameter of cylinder (m)
E - modulus of elasticity (GPa)
EI - energy input (J)
F_n - normal force (N)
FI - fracture index
FR - fracture resistance (rev mg^{-1})
FR_v - volumetric fracture resistance (rev mm^{-3})
H - hardness (MPa)
IA - index of abrasion (mg m^{-2} s^{-1})
IC - index of comminution (mg J^{-1})
K_c - fracture toughness (MPa $m^{-0,5}$)
l - length of edge (mm)
i - rotational speed (s^{-1})
n - number of revolutions
p - pressure (MPa)
R - radius (m)
PC - fraction of pulverized abradant (75 μm)
S - area of surface created by edge chipping (mm^2)
S_A - area of surface exposed to abrasion (m^2)
t - time (s)
t_d - duration of test (s)
T - average integral value of torque (Nm)
v - velocity (m s^{-1})
T_p - peak value of torque (Nm)
T_r - residual value of torque (Nm)
Δm - wear of bar (g)
ΔV - volumetric wear of bar (mm^3)
WR - wear resistance (MJ g^{-1})
α - angular displacement (deg)
σ_r - compressive strengh (MPa)
σ_n - normal stress (MPa)
τ - shear strength (MPa)
τ_p - peak value of shear strength (MPa)
τ_r - residual value of shear strength (MPa)
ø - internal friction angle (deg)
ρ - density (Mg m^{-3})